Drying Technology
Publication details, including instructions for authors and subscription information:
http://www.informaworld.com/smpp/title~content=t713597247

Application of Grey Prediction in a Solar Energy-Assisted Photocatalytic Low-Pressure Drying Process

Ho-Hsien Chen[a]; Chao-Chin Chung[a]; Chih-Hsiang Hsu[a]; Tzou-Chi Huang[a]
[a] Department of Food Science, National Pingtung University of Science and Technology, Pingtung, Taiwan

Online publication date: 15 September 2010

To cite this Article Chen, Ho-Hsien , Chung, Chao-Chin , Hsu, Chih-Hsiang and Huang, Tzou-Chi(2010) 'Application of Grey Prediction in a Solar Energy-Assisted Photocatalytic Low-Pressure Drying Process', Drying Technology, 28: 9, 1097 — 1106
To link to this Article: DOI: 10.1080/07373937.2010.506168
URL: http://dx.doi.org/10.1080/07373937.2010.506168

Drying Technology, 28: 1097–1106, 2010

ISSN: 0737-3937 print/1532-2300 online
DOI: 10.1080/07373937.2010.506168

Taylor & Francis
Taylor & Francis Group

Application of Grey Prediction in a Solar Energy-Assisted Photocatalytic Low-Pressure Drying Process

Ho-Hsien Chen, Chao-Chin Chung, Chih-Hsiang Hsu, and Tzou-Chi Huang
Department of Food Science, National Pingtung University of Science and Technology, Pingtung, Taiwan

An experimental solar energy-assisted photocatalytic low-pressure dryer (SEPLD) for batch food dehydration was developed and tested in an attempt to completely utilize green energy and contribute to reducing greenhouse gas emissions. The dryer consists of high-transmittance glass used to absorb heat from solar radiation, by which means the water content of food products was vaporized and removed using a low-pressure generation system. The performance test, sensory evaluation, and compound analysis showed that the SEPLD had a faster dehydration rate than other drying processes, and samples retained better color and higher amounts of nutrients. Due to the photocatalyst's (TiO_2) action, samples dried using the SEPLD had lower bacterial counts. During the food-drying process, the weight of materials is usually calculated with the drying time to obtain dehydration equations that can be used to further assess the efficiency of the drying equipment and drying performance, such as the drying characteristic curves, drying rate, diffusion coefficient, and so on. However, some information was not easy to obtain during the drying process. We spent a lot of time measuring the water content of a large number of raw materials, especially for those raw materials that were difficult to dry. In this study, some seasonal fruits (pineapple [*Ananas comosus* L. Merrill], tomato [*Lycopersicon esculentum*], and star fruit [*Averhoa carambola* L.]) were selected for the drying tests at 40, 50, and 60°C in the SEPLD. The grey prediction methodology (GPM) was used with water content data to establish the SEPLD drying model, and this was applied to simulate the drying process at different temperatures. The results showed that the accuracy of 60°C drying by GM(1,1) of the GPM was better than the other prediction models. It also indicated that the GPM was a feasible way to simulate the drying process. A patent for the SEPLD was granted and issued in Taiwan.

Keywords Grey prediction methodology (GPM); Pineapple; Solar energy-assisted photocatalytic low-pressure dryer (SEPLD); Star fruit; Tomato

INTRODUCTION

The drying of agricultural products aims to decrease the moisture content to reduce the weight and bulk in order to preserve the food without affecting the quality of the flavor. Transport costs are thereby reduced, and the dried products can be transported to more distant places. Also, due to the increased shelf life of the dried product, it can be sold at appropriate times of the year for a greater profit. Currently in Taiwan, the traditional method of open sun drying is still being used for many agricultural and food products, such as orange peel (used for traditional Chinese medicine), persimmons, Shin-Chu rice noodles, and sakura shrimp (*Sergia lucens* Hansen, a pelagic planktonic shrimp that lives on the sea bottom at 100–300 m in depth). Some characteristic flavors and textures of these products can be generated especially after being exposed to sunlight in the environment at a proper temperature, mild air movement, and low humidity.[1] Without sunlight exposure, the product will have a poor taste or flavor and reduced value.

Various types of solar dryers have been designed to replace open sun drying for reasons of sanitation, quality, and energy savings. Such solar dryers can be classified into direct, indirect, and mixed-mode types that are equipped with solar collectors and operated under ambient conditions.[2] However, the major disadvantages of open sun drying are relatively poor control over meteorological conditions (especially in countries situated in tropical or subtropical areas in which high relative humidities occur in most seasons) and poor sanitary conditions that may affect the drying rate and quality of the dried products. Drying using a hot air dryer may have higher energy costs and also degrade the quality of the product due to chemical reactions during the heating process, leading to browning and loss of fragrance. Consequently, in order to improve the marketability, artificial additives, such as preservatives and color retention agents, may be used. However, consuming too many additives can lead to health problems.

In recent studies, improvements in the drying efficiency and quality of dried products of such solar dryers were proposed. Apart from air drying, Rajkumar et al. developed a laboratory-type vacuum-assisted solar dryer to study the drying kinetics of tomato slices.[3] The apparatus consists mainly of a polycarbonate vacuum bell and a vacuum pump. The study concluded that good quality dried tomato

Correspondence: Tzou-Chi Huang, Department of Food Science, National Pingtung University of Science and Technology, 1, Shuehfu Road, Neipu, Pingtung 912, Taiwan; E-mail: tchuang@mail.npust.edu.tw

slices could be obtained using a vacuum-assisted solar dryer compared to open sun-drying methods. However, concerns about high energy costs for a scaled-up dryer with a vacuum system cannot be ignored, especially for longer-term batch drying processes. Thus, designing a drying system to obtain good quality dried materials while reducing energy consumption and greenhouse gas emissions is still an important task that needs to continue to be investigated, and this was the driving force behind the present study.

Most current drying curve models use a thin-layer drying model and are expressed by an exponential function, because it can simplify and reduce the model's complexity.[4] The drying characteristic curves are calculated using a modified equation as:[4,5]

$$\mathrm{MR} = \frac{M(t) - M_{eq}}{M_0 - M_{eq}} \tag{1}$$

where MR is the moisture ratio, and t is the drying time. The MR determines the initial moisture, M_0; the running moisture change on drying time, $M(t)$; and the equilibrium moisture content, M_{eq}. Exponential models, derived from traditional statistical methods, require large amounts of data, and the thickness of raw materials often restricts the dehydration effect and affects the accuracy of the drying model. These are drawbacks of traditional models.

The traditional research approach in food processing requires precise instrumental analysis or statistical analysis with a large amount of experimental data.[6] It is often the case that data are either insufficient, difficult to collect, or prohibitively expensive.[6] This may impair the functionality of the machine or increase the difficulty of operating in atraditional control system. Grey system theory provides a framework for predicting system responses based on uncertain and incomplete system information.[7] The prediction is obtained by solving an ordinary differential equation (ODE) with model coefficients being updated online to characterize the process dynamics.

Grey theory treats the outputs of a process as variations within a certain range and describes the process as time-varying dynamics confined within a certain range. Unlike the stochastic process theory, which uses statistical regulation, Grey theory uses data aggregation and generation to produce predictions from partially known or random process data.[7] This procedure is called *Grey prediction*, which is commonly used to estimate future system responses based on past and presently known information. Our previous works demonstrated that Grey system theory can be a useful tool for food processing.[8–10] Thus, this work adopted the Grey prediction methodology (GPM) for an experimental type of solar energy-assisted low-pressure dryer (SEPLD) for an agricultural drying process. Energy was provided by high-quality oil using simple yet cheap methods to convert waste animal fat into biodiesel. Also, an evaluation of the quality parameters described above is included in order to demonstrate the advantages of the SEPLD. Because pineapple (*Ananas comosus* L. Merrill), tomato (*Lycopersicon esculentum*), and star fruit (*Averhoa carambola* L.) are the most important tropical fruits in Asia and important economic crops in Taiwan, they were selected as test samples to assess the drying performance of this system.

MATERIALS AND METHODS

Description of the Apparatus

A schematic diagram of the experimental SEPLD associated with the biodiesel generator (3GF-LE, Shanghai Yangke Engine, Shanghai, China, output power 3.3 kW, 240/120 Vac) used as an electrical supply is shown in Fig. 1. SEPLD utilizes the heat from the sun's radiation that passes directly through the drying chamber (20 kg capacity, 0.3 [$L_{\min}$] and 1.1 m [$L_{\max}$] $\times$ 1.1 m [W] $\times$ 0.8 m [H], including 9 trays) as a heat source to dry agriculture products or foods; absorption of solar radiation complements the heat from the electrical heater. The front, side, and top walls of the drying chamber are fitted with high-transmittance glass (3-mm thickness, BK-7, Crylight Photonics, Fujian, China), which allows exposure of the product to solar radiation as an important feature for obtaining high-quality products. The biodiesel generator

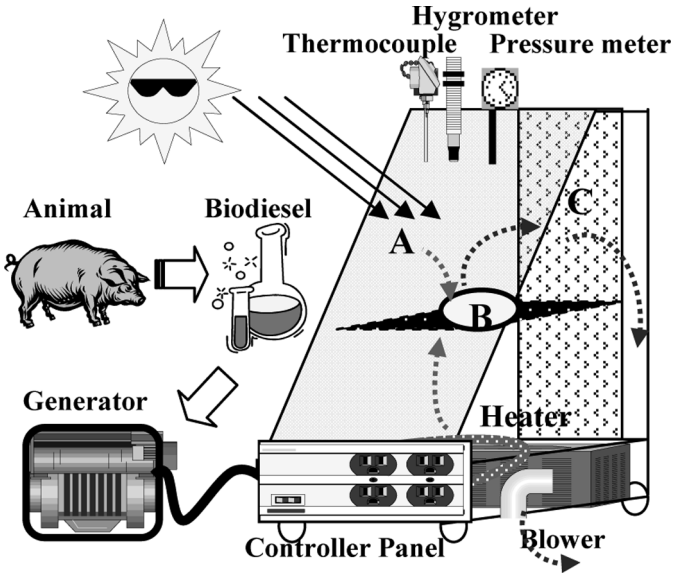

FIG. 1. Schematic diagram of the experimental solar energy-assisted photocatalytic low-pressure dryer (SEPLD). (A) High-transmittance glass, (B) trays, and (C) sieve.

has a display output power of 3.3 kW and a rated output voltage of 240/120 Vac. Animal fat was converted into biodiesel to provide electrical power and generate negative pressure from a high-pressure blower (LG-106A, Serve-Well Enterprise, Taichung, Taiwan). An auxiliary heater (3.5 kW) can be switched on depending on the set temperature and meteorological conditions. In addition, a thin layer of a photocatalyst (food-grade titanium dioxide, TiO_2, ARC-Flash, Taipei, Taiwan) was coated on the inside walls of the glass so that the TiO_2 was catalyzed by ultraviolet waves from sunlight to generate an antimicrobial effect in the drying chamber.

Sensors

Inside the chamber, the temperature was monitored by a controller (SR-T701, CAHO, Shiuan Rong Industrial, Taipei, Taiwan). The pressure meter (model S-10, WIKA Alexander Wiegand, Lawrenceville, GA) has a display range of 250–760 mmHg. The thermal/hygrotransmitter (HTS-801, INS Instrumentation, Taipei, Taiwan) has a display range of 0–100% relative humidity (RH) corresponding to 100°C. The data collected from the load cell is processed by means of a PC to obtain the drying rate of the batch.

Grey Prediction

The prediction is carried out using a Grey model that iterates model parameters to encounter uncertain system variations. Past and present system responses are manipulated with an accumulated generating operation (AGO) to obtain the grey model online. The inverse AGO (IAGO) of the model predicts system responses. Both the AGO and IAGO are presented as ODEs and are manipulated in a discrete time domain. This makes Grey theory easy to implement. The general form of the Grey model is $GM(n,h)$ with n denoting the order of the ODE and h the number of Grey variables. A larger-order n exponentially increases the generation time but might not ensure any improvement in the prediction accuracy.[11] In this work, the $GM(1,1)$ model with a first-order ODE was adopted to predict the drying processes.

For sequence data, $\mathrm{y} = \mathrm{y}[m|m \in N]$, a monotonically increasing AGO sequence of data, $y^{(1)}[k]$, is defined as:

$$y^{(1)}[k] = \sum_{m=k-N+1}^{k} y[m]; \tag{2}$$

where N is a memory horizon defining the length of the historical data to be used in the AGO. For a causal system, the initial value is defined by letting $k = 0$ as:

$$y^{(1)}[0] = y(0). \tag{3}$$

The original sequence data, $y[k]$, can be reconstructed from the AGO sequence using the IAGO manipulation as:

$$y[k] = y^{(1)}[k] - y^{(1)}[k-1]. \tag{4}$$

The resultant AGO increases monotonically in a predictable way for a stable system. Hence, it is reasonable to describe the dynamic behavior of the AGO by a first-order ODE:[7]

$$\frac{dy^{(1)}(t)}{dt} + \alpha y^{(1)}(t) = \xi \tag{5}$$

The adapting coefficient, α, determines how fast the dynamics approach the perturbation input, ξ. Solving and displaying Eq. (5) gives:

$$\hat{y}^{(1)}[k+1] = \left(y[k-N+1] - \frac{\xi}{\alpha}\right)e^{-\alpha(k+1)} + \frac{\xi}{\alpha}. \tag{6}$$

The prediction at the $(k+1)$th step can be estimated using the above derivation:

$$\begin{aligned}\hat{y}[k+1] &= \hat{y}^{(1)}[k+1] - \hat{y}^{(1)}[k] \\ &= (1-e^{-\alpha})\left(y[k-N+1] - \frac{\xi}{\alpha}\right)e^{-\alpha k}.\end{aligned} \tag{7}$$

The differential term of Eq. (5) can be approximated by a discrete form:

$$\frac{dy^{(1)}(t)}{dt} \approx \lim_{T\to 0}\frac{y^{(1)}[k+1] - y^{(1)}[k]}{T} = y[k] \tag{8}$$

with a unit sampling interval, T. The second term on the left-hand side of Eq. (5) can be approximated by the mean value of $y^{(1)}[k]$ and $y^{(1)}[k-1]$. This together with Eq. (8) changes Eq. (5) to:

$$y[k] = -\alpha\frac{y^{(1)}[k+1] - y^{(1)}[k]}{T} + \xi[k]. \tag{9}$$

This representation states that the system response can be predicted one step ahead with the existing AGO data, the adapting coefficients α and the perturbation input ξ. The first term on the right-hand side of Eq. (9) is, in fact, a derivation of the known system response, $y(t)$, by the AGO. It becomes an identification problem of estimating the two unknown coefficients, α and ξ. The least-squares (LSQ) technique was hence employed to identify these two coefficients. The corresponding matrix equation is

$$\hat{\theta} = \begin{bmatrix}\hat{\alpha}\\ \hat{\xi}\end{bmatrix} = (\Phi^{\mathrm{T}}\Phi)^{-1}\Phi^{\mathrm{T}}y \tag{10}$$

where

$$y = [y[k-N+1]y[k-N+2]\ldots y[k]]^{T} \tag{11}$$

and

$$\Phi = \begin{bmatrix} -\frac{1}{2}(y^{(1)}[k-N+1] + y^{(1)}[k-N+2], 1 \\ -\frac{1}{2}(y^{(1)}[k-N+2] + y^{(1)}[k-N+3], 1 \\ \vdots \\ -\frac{1}{2}(y^{(1)}[k-1] + y^{(2)}[k] \qquad , 1 \end{bmatrix} \quad (12)$$

The Grey model prediction is a local curve-fitting extrapolation scheme. At least four data sets are required by the predictor (7) to obtain a reasonably accurate prediction.[7] A system in a steady state fills the transition matrix of Eq. (10) with the same response values. This incurs numerical singularity in matrix manipulation and nulls the $\hat{\alpha}$ and $\hat{\xi}$ values. Freezing the LSQ identification when the system is in a steady state resolves the singularity problem.[11] Substituting the estimates into Eq. (7) works out the prediction data for the drying process. To determine the efficiency of the proposed forecasting model, this study adopted the residual error test method to compare the forecasted and actual values. The formula is as follows:

$$e[k] = \left| \frac{y^{(1)}[k+1] - \hat{y}^{(1)}[k+1]}{y^{(1)}[k+1]} \right| \times 100\%. \quad (13)$$

The accuracy is $1 - e[k]$, and the model is considered useful if the average accuracy exceeds 90%.

Mathematical Modeling of the Drying Curves

The transport of water during the food dehydration process takes place predominately in the falling rate period. This is controlled by the liquid diffusion mechanism and can be described by Fick's law, when radial diffusion is considered. Crank[12] first gave analytical solutions to Fick's equation for various geometries (sphere, cylinder, and rectangular plate), which were later used by many researchers to describe the drying phenomena of various foodstuffs.[12,13] Thin-layer drying models, which describe the drying process, can be distinguished into three main categories, namely, the theoretical, semitheoretical, and fully empirical.[14] The major difference between these groups is that theoretical models suggest that moisture transport is mainly controlled by internal resistance mechanisms, whereas the other two consider only external resistance. The basic equation most commonly used to describe the thin-layer drying process is similar to Newton's law for cooling and incorporates a single drying constant (k) for the combined effect of the various existing transport phenomena. It was first suggested by Lewis's work and has the general form:[15]

$$\mathrm{MR} = \exp(-k \times t) \quad (14)$$

Other drying models with a similar approach are Henderson and Pabis' model:[16]

$$\mathrm{MR} = a_{\mathrm{HP}} \times \exp(-k \times t) \quad (15)$$

and the Page model:[17]

$$\mathrm{MR} = a_{\mathrm{P}} \times \exp(-k \times t^n) \quad (16)$$

which were introduced for the thin-layer drying of fruits.

Sample Preparation

Fresh pineapple (Tainung 17, Tainan, Taiwan), tomato (Taichung AVRDC no. 10), and star fruit (Tainung no. 2, Taiwan) purchased from a local market in Pingtung City, southern Taiwan, were used as the samples to be dried. After peeling and coring, samples were cut into slices about 15–20 mm thick, and 4.80–5.00 kg of samples was prepared per batch at 40–45°C by SEPLD drying (from June to September in Taiwan), 40°C low-temperature air drying, and 60°C hot air drying, respectively. The drying process was terminated when the water activity (A_w) reached 0.4. The average moisture content of the material taken from inside the drying chamber was evaluated by an Association of Analytical Chemists (AOAC) method.[18,19]

Water Activity

Water activity (A_w) was measured with a water activity meter (AQUA LAB CX-2, Decagon Devices, Pullman, WA). After beginning the experiment, a sample was removed from the drying cabinet, and the A_w was measured every hour using a water activity meter.

Color Assessment

The degree of browning, resulting from both enzymatic and nonenzymatic browning reactions, was mainly determined by the induced color change during drying. Hunter $L^*a^*b^*$ values of dried samples were obtained using a color difference meter (CDM-08, Laiko, Tokyo, Japan). Three replicates were used for each drying treatment. The L^* value was used as an indicator of brightness, a^* to indicate chromaticity on a green (−) to red (+) axis (the higher the a^* value, the closer it is to green), and b^* to indicate chromaticity on a blue (−) to yellow (+) axis (the higher the b^* value, the closer it is to yellow).[20] However, it is also useful to convert the numerical values of L^*, a^*, and b^* into a white index (WI) value. The highest value of the WI represents the lowest degree of browning, which was defined as follows:

$$\mathrm{WI} = 100 - ((100 - L)^2 + a^2 + b^2)^{1/2}. \quad (17)$$

Microstructure of the Samples

Changes in the microstructure of samples dried by hot air, low-temperature air, and SEPLD were observed using a scanning electron microscope (SEM, S-4300, Hitachi, Tokyo, Japan). A piece of the sample slice was taken along its cross-sectional axis, attached to an SEM stub, coated with a gold layer using a vacuum sputter-coater, and photographed at an accelerator potential of 10 kV. The locations of the dried pineapple slices examined were the surface and cross section.

Total Bacterial Count

Bacteriological analyses were carried out in triplicate on 10 g of raw dried samples that was blended with 90 mL of sterile water as described in the bacteriological analytical manual.[1] Pour plates were prepared from 10-fold dilutions in potato dextrose agar (PDA, Difco, Sparks, MD) for mold and yeast counts and plate count agar (PCA, Difco) for bacterial counts. Counts were made after incubation at 35°C for 48 h.

Vitamin C and Bromelain Analyses

Vitamin C levels were measured by spectrophotometry (U-2001 model, Hitachi). According to the AOAC method as described by Nursal and Yücecan (2000), 2,6-dichlorophenolindophenol dye is reduced by ascorbic acid. Bromelain levels were measured by spectrophotometry (U-2001 model) following the AOAC procedure.[18]

Computational Fluid Dynamics Analysis

The flow field inside the SEPLD chamber is governed by Reynolds-averaged equations of continuity and momentum for steady, incompressible flow. The governing equations with the boundary equations were numerically solved using the well-validated commercial computational fluid dynamics (CFD) software, FLUENT (Fluent v. 6.1.2, Santa Clara, CA).[22–25] The finite-volume difference scheme, segregated solver, and implicit technique were used to solve the algebraic equations formed from discriminating a closed set of equations. In order to ensure good resolution of the numerical results, the computational domain was discretely calculated with structural hexahedral meshes containing approximately 600,000 cells.

Statistical Analysis

Analysis of variance (ANOVA) was used to investigate the significance of the influence and confidence of the drying process parameters on the performance. A regression analysis of the experimental data was obtained using SAS 8.2 (Statistical Analysis System, Cary, NC).[26] Duncan's multiple range test was used to compare the difference between means at a probability level of <0.05.[26–28]

RESULTS AND DISCUSSION

Simulation and Mechanism

Figure 2 illustrates the uniform vapor flow line distribution in the SEPLD. Vapor forcefully flowed out through holes at the back of the dryer due to very strong suction by the high-pressure blower. Figure 3 shows the mechanism of vapor flow, for which the initial states were T_A of 45°C and P_A of 1 atm at location A. Reducing the pressure to, say, 0.868 atm at location B would speed up the removal of saturated moisture around the surface of samples and bring moisture from inside of the materials to the surface. During this stage of moisture removal, the temperature of the samples dropped to a T_C of 40°C.

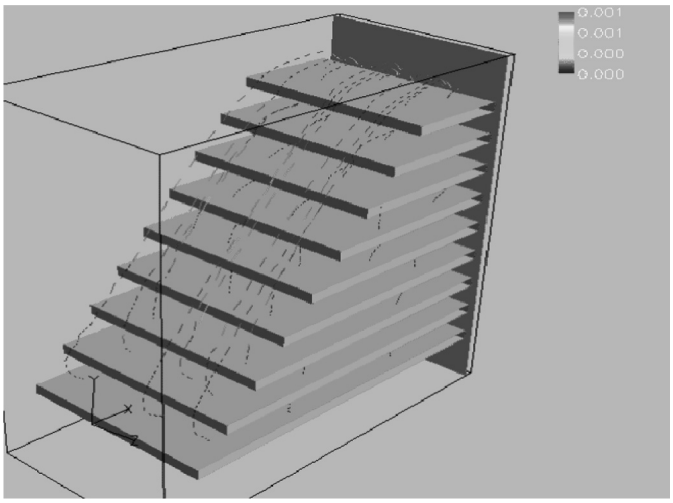

FIG. 2. CFD simulation of dynamic vapor flow lines.

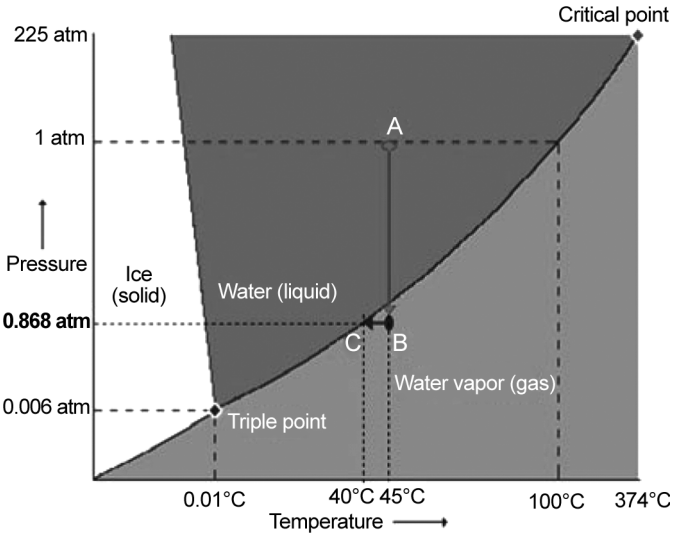

FIG. 3. Phase diagram analysis of the solar energy-assisted photocatalyst low-pressure dryer (SEPLD).

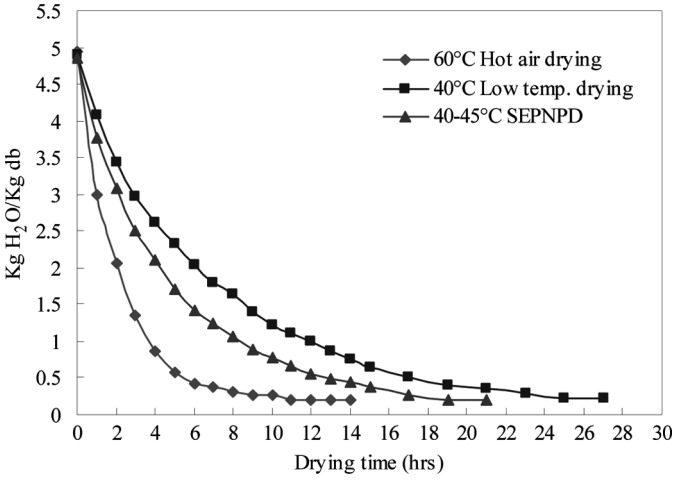

FIG. 4. Drying rates of different drying processes.

TABLE 1
Water activity of pineapple slices under different drying processes

Sample	Water content (%)	Water activity
Fresh fruit	0.85 ± 0.06^a	0.97 ± 0.02^a
40°C low-temp. air	0.18 ± 0.03^b	0.39 ± 0.03^b
40–45°C SEPLD	0.17 ± 0.02^b	0.37 ± 0.04^b
60°C hot air	0.17 ± 0.03^b	0.36 ± 0.04^b

^{ab}Means with the same letters in a column do not significantly differ from each other (by Duncan's multiple range test, $p < 0.05$).

Drying Performance

A water content curve versus time is shown in Fig. 4, and the water activities of pineapple slices under different drying processes are shown in Table 1. Results show that 60°C hot air drying had the fastest drying rate. It took 11 h to reach a moisture content of 0.21 kg H_2O/kg dry basis at a water activity of 0.36. For SEPLD drying, it took 17 h to reach a moisture content from 4.95 to 0.21 kg H_2O/kg dry basis, whereas low-temperature drying took 27 h to reach the same value.

Grey Prediction System Implementation

The GPM strategy was implemented using Visual Basic (Version 6, Microsoft Co., USA) to construct a graphical user interface, which is shown in Fig. 5. A sampling period of 1 h was chosen among several candidates undergoing tentative experiments, as a forecast of drying system responsiveness. Results were compared with four, five, six, and seven input data collected for modeling. Results showed that a four-data slide model could be successfully applied to regression problems of drying processes (accuracy of the GMP > 90%, $R^2 = 99.92\%$, root mean square error [RMSE] of 0.57%).

Comparisons of Various Prediction Systems

The GPM defined in Eq. (6), the Lewis model in Eq. (14), the Henderson and Pabis model in Eq. (15), and the Page model in Eq. (16) were studied for various drying processes, and the results are shown in Fig. 6. The results showed that the Lewis model equations were as follows.

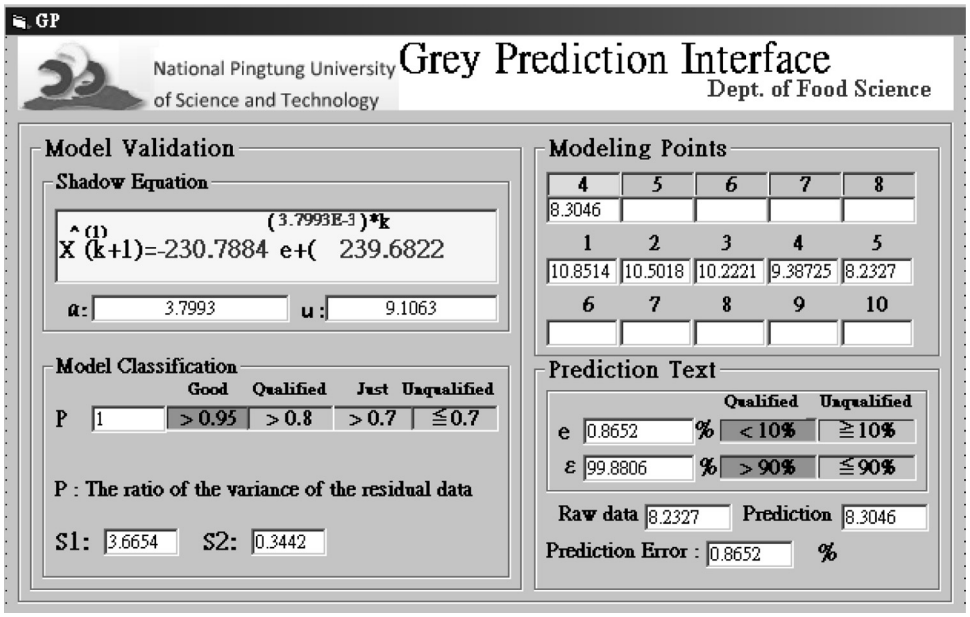

FIG. 5. Graphical user interface of Grey prediction used for the drying process.

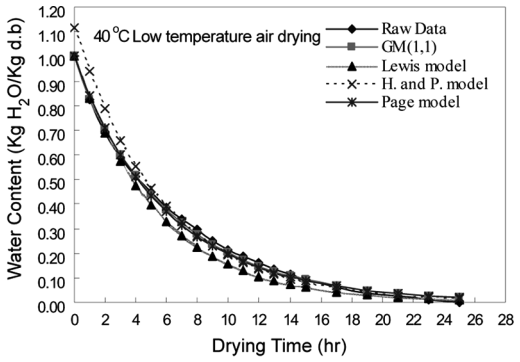

(a)

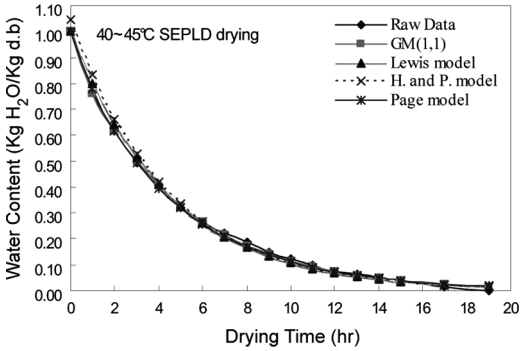

(b)

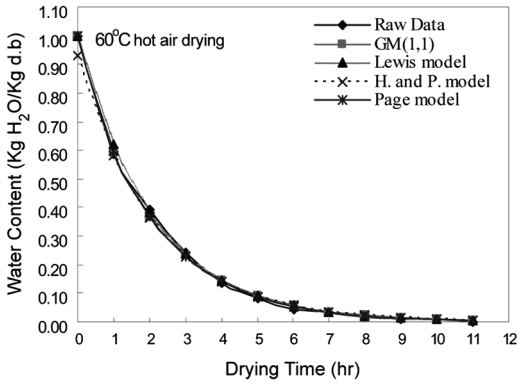

(c)

FIG. 6. Different prediction model systems of drying characteristic curves under different drying processes: (a) 40°C low-temperature air drying, (b) 40–45°C solar energy-assisted photocatalytic low-pressure drying, and (c) 60°C hot air drying.

- Lewis model equation:
  - for low-temperature drying (40°C)

$$\mathrm{MR} = \exp(-0.1862 \cdot t)\ (R^2 = 99.08\%, \mathrm{RMSE} = 4.22\%) \quad (18)$$

for SEPLD drying (40–45°C)

$$\mathrm{MR} = \exp(-0.2237 \cdot t)\ (R^2 = 99.82\%, \mathrm{RMSE} = 1.41\%) \quad (19)$$

for hot air drying (60°C)

$$\mathrm{MR} = \exp(-0.4787 \cdot t)\ (R^2 = 99.88\%, \mathrm{RMSE} = 1.13\%) \quad (20)$$

- Henderson and Pabis model equation:
  - for low-temperature drying (40°C)

$$\mathrm{MR} = 1.1188 \cdot \exp(-0.1761 \cdot t)\ (R^2 = 99.39\%, \mathrm{RMSE} = 4.79\%) \quad (21)$$

for SEPLD drying (40–45°C)

$$\mathrm{MR} = 0.2277 \cdot \exp(-1.0458 \cdot t)\ (R^2 = 99.80\%, \mathrm{RMSE} = 2.55\%) \quad (22)$$

for hot air drying (60°C)

$$\mathrm{MR} = 0.9321 \cdot \exp(-0.4686 \cdot t)\ (R^2 = 99.86\%, \mathrm{RMSE} = 2.18\%) \quad (23)$$

- Page model equation:
  - for low-temperature drying (40°C)

$$\mathrm{MR} = \exp(-0.1771 \cdot t^{0.9641})\ (R^2 = 99.69\%, \mathrm{RMSE} = 1.62\%) \quad (24)$$

for SEPLD drying (40–45°C)

$$\mathrm{MR} = 0.2277 \cdot \exp(-1.0458 \cdot t)\ (R^2 = 99.88\%, \mathrm{RMSE} = 0.96\%) \quad (25)$$

for hot air drying (60°C)

$$\mathrm{MR} = 0.9321 \cdot \exp(-0.4686 \cdot t)\ (R^2 = 99.89\%, \mathrm{RMSE} = 0.97\%) \quad (26)$$

The results of the GM(1,1) four-data slide model for low-temperature drying (40°C) were $R^2 = 99.80\%$ and RMSE = 1.25%; for SEPLD drying (40–45°C), $R^2 = 99.93\%$ and RMSE = 0.74%; and for hot air drying (60°C), $R^2 = 99.92\%$ and RMSE = 0.86%.

Color Assessment

Figure 7 shows that dried pineapple slices had significant color differences resulting from the browning reaction under the three drying methods. The constant 60°C drying using the hot air dryer resulted in a deeper brown color than the 40°C low-temperature air drying and SEPLD drying. Table 2 shows the Hunter $L^*a^*b^*$ and WI values for pineapple slices with different drying processes. The results showed that 60°C hot air drying had the highest values of both a^* and b^* and the lowest L^* value (L^* 53.54 units/g, a^* 7.64 units/g, b^* 36.04 units/g, $p < 0.05$), which significantly

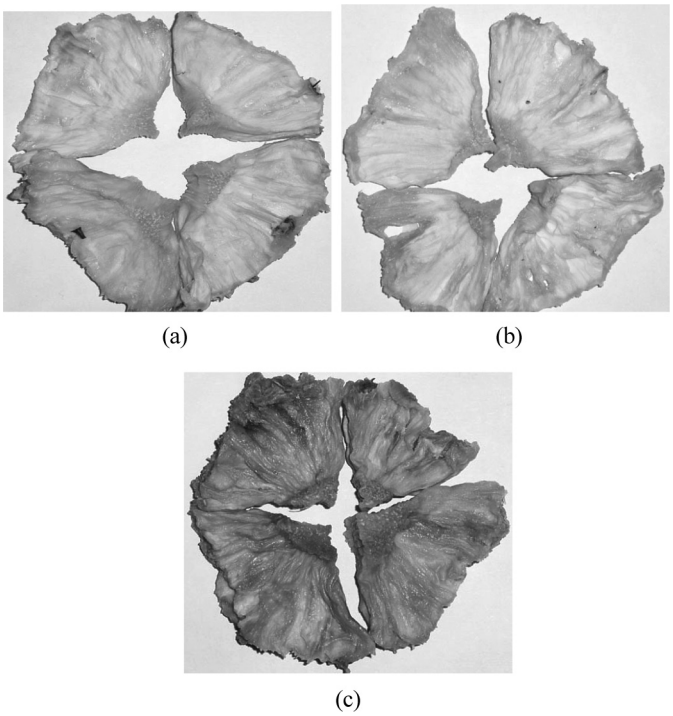

FIG. 7. (a) A dried pineapple slice with a dim color under low-temperature drying (40°C); (b) a dried pineapple slice with a bright color under solar energy-assisted photocatalytic low-pressure drying (40–45°C); and (c) a dried pineapple slice with brown color under hot air drying (60°C).

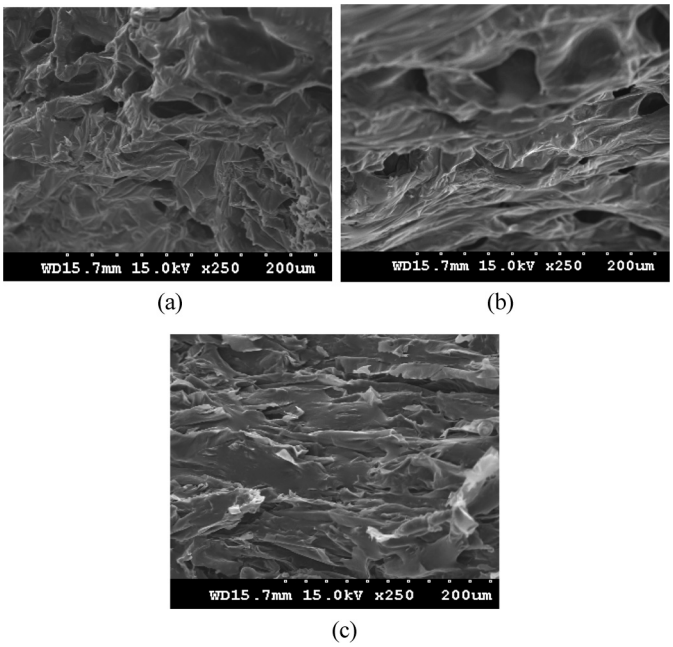

FIG. 8. SEM images of pineapple slices after different drying processes: (a) 40°C low-temperature air, (b) 40°C solar energy-assisted photocatalytic low-pressure drying, and (c) 60°C hot air.

differed from the other drying processes. In addition, the lowest WI value (40.71 units/g, $p < 0.05$) was also found with hot air drying at 60°C due to browning reactions. Low-temperature drying at 40–45°C by SEPLD (L^* 65.71 units/g, a^* 1.26 units/g, b^* 25.57 units/g) retained the primary colors, and the color was closer to that of fresh pineapple (L^* 65.78 units/g, a^* 0.56 units/g, b^* 28.30 units/g) than the low-temperature air-drying process (L^* 66.77 units/g, a^* 1.53 units/g, b^* 33.21 units/g). Also, a higher WI value (57.2 units/g) and less browning were found with the SEPLD. Longer drying times in this study may have degraded the quality of the dried samples.

Microstructure of Samples

Figure 8 shows images of dried pineapple slices observed (250×) with the drying conditions of 40°C low-temperature air, 40–45°C SEPLD, and 60°C hot air drying processes. It was found that the samples maintained the original tissues and had porous structures with low-temperature drying, as shown in Figs. 8a and 8b. A high drying temperature led to tissue shrinkage, as shown in Fig. 8c.

Vitamin C and Bromelain

Table 3 indicates that about 86.71% of the vitamin C was lost in the 60°C hot air drying process (from 1,736.36 to 230.77 mg/kg dry basis). For SEPLD, 53.32% of the vitamin C (925.87 mg/kg dry basis) remained, and about 44.13% of the vitamin C (766.18 mg/kg dry basis) remained with low-temperature drying. For protease enzymes, similar results for SEPLD were obtained because

TABLE 2
Hunter $L^*a^*b^*$ values and the white index (WI) of pineapple slices under different drying processes

Sample	L^* value (units/g)	a^* value (units/g)	b^* value (units/g)	WI value (units/g)
Fresh fruit	65.78 ± 0.05^b	0.56 ± 0.08^d	28.30 ± 0.04^c	55.59 ± 0.06^b
40°C low-temp. air	66.77 ± 0.05^a	1.53 ± 0.08^b	33.21 ± 0.04^b	52.99 ± 0.06^c
40–45°C SEPLD	65.71 ± 0.08^b	1.26 ± 0.06^c	25.57 ± 0.08^c	57.21 ± 0.06^a
60°C hot air	53.54 ± 0.09^c	7.64 ± 0.01^a	36.04 ± 0.06^a	40.71 ± 0.08^d

[abcd]Means with the same letters in a column do not significantly differ from each other (Duncan's multiple range test, $p < 0.05$).

TABLE 3
Vitamin C and protease activities of pineapple slices under different drying processes

Sample	Vitamin C (mg/kg dry basis)	Bromelain (U/kg dry basis)
Fresh fruit	$1{,}736.36 \pm 0.14^a$	$1{,}298.91 \pm 0.05^a$
45°C low-temp. air	766.18 ± 0.09^c	305.06 ± 0.03^c
40–45°C SEPLD	925.87 ± 0.12^b	372.99 ± 0.08^b
60°C hot air	230.77 ± 0.01^d	ND

^{abcd}Means with the same letters in a column do not significantly differ from each other (Duncan's multiple range test, $p < 0.05$).

it could maintain about 28.72% of the bromelain (from 1,298.91 to 372.99 U/kg dry basis) which was higher than that with low-temperature air drying (305.06 U/kg dry basis). However, no pineapple enzymes were detected after 60°C hot air drying.

Bactericidal Effect of the Photocatalyst

The average total count of the five samples located in the drying chamber was from 21 (before being coated with the photocatalyst) to 3 colony-forming units (CFU)/g (after being coated with the photocatalyst), which meets the specification of a CNS working environment (of <15 CFU/g). Some batch operations even showed no detection of bacteria. The results also confirmed that coating the drying chamber with a photocatalyst can have an antimicrobial effect compared to other drying processes (Table 4).

Feasibility of GPM Predictions for Drying Other Fruits

The study used GM(1,1) to forecast tomato (Taichung AVRDC No. 10) and star fruit (Tainung No. 2, Taiwan) drying processes, and the results are shown in Table 5. The accuracy of the drying process by the four-point Grey prediction was better than other drying models with an exponential model for prediction. It also indicated that using the Grey prediction of four-point modeling is a feasible way to simulate the drying process.

TABLE 4
Total bacteria counts of pineapple slices under different drying processes

Sample	Total bacteria count (CFU/g)
40°C low-temperature air	$3{,}500^a$
40°C SEPLD (without the photocatalyst)	$2{,}500^b$
40–45°C SEPLD (with the photocatalyst)	$<10^d$
60°C hot air	$<100^c$

^{abcd}Means with the same letter in a column do not significantly differ from each other (Duncan's multiple range test, $p < 0.05$).

TABLE 5
Accuracy of different prediction models for pineapple, tomato, and star fruit with solar energy-assisted photocatalytic low-pressure drying (SEPLD) processes

Prediction model	Root mean square error (RMSE)	Correlation coefficient R^2
GM(1,1)	0.058	0.9778
Lewis model	0.103	0.9216
Henderson and Pabis model	0.093	0.9419
Page model	0.064	0.9763

CONCLUSIONS

In this research, an experimental solar energy-assisted photocatalytic low-pressure dryer was developed to utilize solar radiation as a heat complement and was successfully used to dry pineapple slices. This is a new solar dryer design incorporating a high-pressure blower, a drying cabinet with transparent glass, and a photocatalyst (TiO_2) coating used to produce an antimicrobial effect. Pineapple slices dried in the SEPLD retained more vitamin C and enzyme protein activity compared to samples dried in 60°C hot air or 40°C low-temperature air drying. The SEPLD was proven to produce high-quality dried products in terms of hygiene, appearance, active compounds that would raise the added value of the products, and lower production costs. The accuracy of the GM(1,1) model used for predicting the drying process based on four-point data was better than the other exponential models. It was also indicated that Grey prediction of four-point modeling is a feasible way to simulate the drying process. The SEPLD has already been granted a patent[29] from the Intellectual Property Office, Taiwan.

ACKNOWLEDGMENTS

This work was supported by a grant (NSC-94-2622-E-020-001) from the National Science Council, Taiwan.

REFERENCES

1. Chen, H.H.; Hernandez, C.E.; Huang, T.C. A study of the drying effect on lemon slices using a closed-type solar dryer. Solar Energy **2005**, *78*, 97–103.
2. Chen, H.H.; Huang, T.C.; Tsai, C.H. Development and performance analysis of a new solar energy-assisted photocatalytic dryer. Drying Technology **2008**, *26*, 503–507.
3. Rajkumar, P.; Kulanthaisami, S.; Raghavan, G.S.V.; Gariepy, Y.; Orsat, V. Drying kinetics of tomato slices in vacuum assisted solar and open sun drying methods. Drying Technology **2007**, *25*, 1349–1357.

4. Pahlavanzadeh, H.; Basiri, A.; Zarrabi, M. Determination of parameters and pretreatment solution for grape drying. Drying Technology **2001**, *19* (1), 217–226.
5. Babalis, S.J.; Papanicolaou, E.; Kyriakis, N.; Belessiotis, V.G. Evaluation of thin-layer drying models for describing drying kinetics of figs (*Ficus carica*). Journal of Food Engineering **2006**, *75* (2), 205–214.
6. Odetunji, O.A.; Kehinde, O.O. Computer simulation of fuzzy control system for *gari* fermentation plant. Journal of Food Engineering **2005**, *68*, 197–207.
7. Deng, J. *Grey Theory Basis*; Huazhong University of Science and Technology: Beijing, China, 2002.
8. Chen, H.H.; Tsai, P.J.; Chen, S.H.; Su, Y.M.; Chung, C.C.; Huang, T.C. Grey relational analysis of dried roselle (*Hibiscus sabdariffa* L.). Journal of Food Processing and Preservation **2005**, *29*, 228–245.
9. Chung, C.C.; Chen, H.H.; Hsieh, P.C. Optimization of the *Monascus purpureus* fermentation process based on multiple performance characteristics. International Journal of Grey System **2008**, *11*, 85–96.
10. Chung, C.C.; Chen, H.H.; Ting, C.H. Grey prediction fuzzy control for pH processes in the food industry. Journal of Food Engineering **2010**, *96*, 575–582.
11. Lian, R.J.; Lin, B.F.; Huang, J.H. A grey prediction fuzzy controller for constant cutting force in turning. International Journal of Machine Tools and Manufacture **2005**, *45*, 1047–1056.
12. Crank, J. *Mathematics of Diffusion*, 2nd Ed.; Oxford University Press: London, 1975.
13. Wani, A.A.; Sogi, D.S.; Shivhare, U.S.; Ahmed, I.; Kaur, D. Moisture adsorption isotherms of watermelon seeds and kernels. Drying Technology **2006**, *24*, 99–104.
14. Babalis, S.J.; Papanicolaou, E.; Kyriakis, N.; Belessiotis, V.G. Evaluation of thin-layer drying models for describing drying kinetics of figs (*Ficus carica*). Journal of Food Engineering **2006**, *75* (2), 205–214.
15. Lewis, W.K. The rate of drying of solid materials. Industrial Engineering Chemistry **1921**, *13*, 427–432.
16. Henderson, S.M.; Pabis, S. Grain drying theory: Temperature effect on drying coefficient. Journal of Agricultural Engineering Research **1961**, *6*, 169–174.
17. Page, G.E. Factors influencing the maximum rates of air drying shelled corn in thin layers, M.Sc. Thesis, Purdue University: Tippecanoe, IN, 1949.
18. AOAC. *Official Methods of Analysis*, 16th Ed.; AOAC International: Washington, DC, 1995.
19. Derdour, L.; Desmorieux, H.; Andrieu, J. Determination and interpretation of the critical moisture content (C.M.C.) and the internal moisture content profile during the constant drying rate period. Drying Technology **1998**, *16* (3), 813–824.
20. Francis, F. Quality as influenced by color. Food Quality and Preference **1995**, *6*, 149–155.
21. Nursal, B.; Yücecan, S. Vitamin C losses in some frozen vegetables due to various cooking methods. Nahrung, **2000**, *44* (6): 451–453.
22. FLUENT. *User's Guide*; FLUENT: Lebanon, NH, 2005.
23. Bacelos, M.S.; Spitzner Neto, P.I.; Silveira, A.M.; Freire, J.T. Analysis of fluid dynamics behavior of conical spouted bed in presence of pastes. Drying Technology **2005**, *23* (3), 427–453.
24. Renaud, M.; Thibault, J.; Alvarez, P.I. Influence of solids moisture content on the average residence time in a rotary dryer. Drying Technology **2001**, *19* (9), 2131–2150.
25. Reyes, A.; Diaz, G.; Blasco, R. Slurry drying in gas-particle contactors: Fluid-dynamics and capacity analysis. Drying Technology **1998**, *16* (1), 217–233.
26. DiIorio, F.C. *SAS® Applications Programming: A Gentle Introduction*; Duxbury Press: Belmont, CA, 1991.
27. Cassini, A.S.; Marczak, L.D.F.; Noreña, C.P.Z. Drying characteristics of textured soy protein: A comparison between three different products. Drying Technology **2007**, *25* (12), 2047–2054.
28. Petersen, J.N. Analysis of batch drying data using SAS. Drying Technology **1986**, *4* (3), 319–330.
29. Chen, H.H.; Huang, T.C.; Tsai, F.L. Inventors: National Pingtung University of Science and Technology, assignee. Solar Energy Assisted Vacuum Dryer. Taiwan Patent I288810, October 21, 2007.